batteries

MDPI

Communication

Electrochemical Studies of Metal Phthalocyanines as Alternative Cathodes for Aqueous Zinc Batteries in "Water-in-Salt" Electrolytes

Wentao Hou [1], Andres Eduardo Araujo-Correa [1], Shen Qiu [1,*], Crystal Otero Velez [1], Yamna D. Acosta-Tejada [2], Lexis N. Feliz-Hernández [2], Karilys González-Nieves [2], Gerardo Morell [3,*], Dalice M. Piñero Cruz [1,*] and Xianyong Wu [1,*]

[1] Department of Chemistry, University of Puerto Rico-Rio Piedras, San Juan, PR 00925-2537, USA; wentao.hou@upr.edu (W.H.); andres.araujo@upr.edu (A.E.A.-C.); crystal.otero1@upr.edu (C.O.V.)
[2] Department of Natural Sciences, University of Puerto Rico-Carolina, Carolina, PR 00984-4800, USA; yamna.acosta@upr.edu (Y.D.A.-T.); lexis.feliz@upr.edu (L.N.F.-H.); karilys.gonzalez@upr.edu (K.G.-N.)
[3] Department of Physics, University of Puerto Rico-Rio Piedras, San Juan, PR 00925-2537, USA
* Correspondence: shen.qiu@upr.edu (S.Q.); gerardo.morell@upr.edu (G.M.); dalice.pinero@upr.edu (D.M.P.C.); xianyong.wu@upr.edu (X.W.)

Abstract: Aqueous zinc batteries are emerging technologies for energy storage, owing to their high safety, high energy, and low cost. Among them, the development of low-cost and long-cycling cathode materials is of crucial importance. Currently, Zn-ion cathodes are heavily centered on metal-based inorganic materials and carbon-based organic materials; however, the metal–organic compounds remain largely overlooked. Herein, we report the electrochemical performance of metal phthalocyanines, a large group of underexplored compounds, as alternative cathode materials for aqueous zinc batteries. We discover that the selection of transition metal plays a vital role in affecting the electrochemical properties. Among them, iron phthalocyanine exhibits the most promising performance, with a reasonable capacity (~60 mAh g^{-1}), a feasible voltage (~1.1 V), and the longest cycling (550 cycles). The optimal performance partly results from the utilization of zinc chloride "water-in-salt" electrolyte, which effectively mitigates material dissolution and enhances battery performance. Consequently, iron phthalocyanine holds promise as an inexpensive and cycle-stable cathode for aqueous zinc batteries.

Keywords: metal phthalocyanines; zinc batteries; aqueous electrolytes; water-in-salt electrolytes; cathode

Academic Editors: Dongliang Chao and Seung-Wan Song

Received: 25 January 2025
Revised: 13 February 2025
Accepted: 20 February 2025
Published: 22 February 2025

Citation: Hou, W.; Araujo-Correa, A.E.; Qiu, S.; Velez, C.O.; Acosta-Tejada, Y.D.; Feliz-Hernández, L.N.; González-Nieves, K.; Morell, G.; Piñero Cruz, D.M.; Wu, X. Electrochemical Studies of Metal Phthalocyanines as Alternative Cathodes for Aqueous Zinc Batteries in "Water-in-Salt" Electrolytes. *Batteries* **2025**, *11*, 88. https://doi.org/10.3390/batteries11030088

1. Introduction

The development of advanced batteries is essential for renewable and sustainable energy storage [1]. Lithium-ion batteries (LIBs) have been widely used in daily life, but limitations, such as elemental scarcity, high costs, and safety concerns (e.g., fires and explosions), have concurrently restricted their applications [2]. Recently, aqueous batteries have gained increasing attention as competitive alternatives for energy storage, due to their high abundance, low cost, non-flammability, and environmental friendliness [3–5]. Furthermore, aqueous electrolytes have 1–2 orders of magnitude higher ionic conductivity than non-aqueous counterparts, which is advantageous for high-power applications [6,7]. Among these systems, aqueous zinc (Zn) batteries have emerged as one of the most promising candidates, due to the high capacity (820 mAh g^{-1}), low potential (−0.76 V vs. standard hydrogen electrode), cost-effectiveness, and non-toxicity of the Zn metal [8,9].

To advance aqueous Zn batteries, it is critical to develop appropriate cathode materials with low cost, high abundance, and long cycling life. Currently, various cathode materials have been investigated, which primarily fall into two categories: (1) inorganic compounds, such as metal oxides [10], phosphates [11], sulfides [12], halogens [13–15], and hexacyanoferrates [16], and (2) organic materials, including small organic molecules [17] and polymers [18]. In general, inorganic materials offer advantages like high tap density, good electronic conductivity, and stable crystal structures, while organic materials provide structural flexibility and molecule-level designability to fine-tune battery performance. However, much less attention has been paid to metal–organic compounds, which can potentially inherit the redox capabilities of transition metals and the structural flexibility of organic groups. Although metal–organic frameworks (MOFs) have been investigated for Zn-ion batteries [19–21], their complex synthesis often results in high material costs. Consequently, it is of significant interest to identify simpler and more cost-effective metal–organic compounds for Zn-ion batteries.

Metal phthalocyanines (MPcs) are organic macrocyclic compounds with a planar conjugated structure [22]. The Pc macrocycle possesses a central cavity that allows them the coordination of diverse ion metals [22,23]. The nature of the coordinated metal can directly affect the optical and conductive properties of the material. MPcs have been widely explored in numerous applications (gas sensors, optical sensors, catalysis, etc.), showing good conductivity and great structural stability [12,24–26]. Furthermore, they are promising candidates for battery applications, due to their unique structural properties and ability to perform reversible redox reactions [27,28]. In addition, the conjugated nature of MPcs facilitates electron transfer, and the choice of the central metal ion (e.g., Co, Fe, Mn, or Cu) allows fine-tuning of battery voltages and capacities [29–31]. Finally, MPc materials are low-cost and amenable to scalable synthesis, making them attractive alternatives to more expensive materials like MOFs.

Despite these attractive merits, the application of MPcs in aqueous Zn batteries remains limited. Recently, Yun et al. investigated several MPcs for flexible Zn batteries [32], including iron, cobalt, nickel, and vanadium-based compounds. Among these, iron phthalocyanine exhibited the highest capacity but suffered from a low voltage (~0.6 V) and a short cycling life (100 cycles). These limitations were likely attributed to material dissolution in conventional 1 M $ZnSO_4$ aqueous electrolytes. It is known that the optimization of electrolytes can effectively enhance the electrode performance [33,34]. In this regard, concentrated and/or "water-in-salt" (WiS) electrolytes have emerged as promising options for aqueous batteries [35–37], which not only impact the electrode redox potentials but also improve the cycling performance. However, to our knowledge, the use of MPc compounds in Zn-based WiS electrolytes has not been reported.

Herein, we evaluated the electrochemical performance of various MPcs (iron, copper, nickel, and cobalt) in a zinc chloride ($ZnCl_2$) WiS electrolyte. Among these compounds, iron phthalocyanine (Fe-Pc) demonstrated the most promising performance, with the highest voltage and longest cycling life. Compared with the literature reports, Fe-Pc also exhibited improved battery voltage and cycling performance. Specifically, it delivered a reasonable voltage of ~1.1 V, a high-rate capability of 1500 mA g^{-1}, and a long lifespan of 550 cycles. This work highlights a promising approach to developing inexpensive and long-cycling cathodes for aqueous Zn batteries.

2. Materials and Methods

2.1. Materials

Zinc chloride (≥98% purity), iron acetate (98% purity), cobalt acetate (98% purity), and the commercial nickel phthalocyanine were purchased from Sigma Aldrich (St. Louis,

MO, USA). The copper chloride (98% purity) was from Alfa Aesar (Ward Hill, MA, USA). The high-purity titanium foil (0.03 mm thickness) was the Futt brand (Chongqing rejiapa e-commerce Co.,ltd, China). The zinc foil (99.99% purity, 0.1 mm thickness) was purchased from Amazon (Seattle, WA, USA). All chemicals and solvents were obtained from commercial suppliers and used without further purification.

To synthesize MPc materials (M = Fe, Cu, and Co), we used solid-state reaction methods (Figure S1). We took the phthalonitrile (the precursor) and the corresponding salt (iron acetate, copper chloride, and cobalt acetate) via the mass ratio of 4 to 1.3, Then, we added them in a vial sealed under an inert atmosphere. Subsequently, they were placed in a sand bath at 250 °C for 3 h.

To evaluate the particle size effect on the battery performance, we ball-milled the Fe-Pc sample for 4 h.

2.2. Materials Characterizations

X-ray diffraction (XRD) patterns of these cathode materials were collected on the Rigaku SuperNova (Woodlands, TX, USA) equipped with a HyPix3000 X-ray detector and CuKα radiation source (λ = 1.5406 Å). Scanning electron microscopy (SEM) images and energy dispersive X-ray spectra (EDS) mapping results were recorded at a field emission scanning electron microscope (SEM, JEOL, JSM-6480LV, Peabody, MA, USA).

2.3. Electrode Preparation

The working electrode was prepared by mixing the active material (Fe-Pc, Cu-Pc, Co-Pc, Ni-Pc), Ketjen black carbon, and polyvinylidene fluoride (PVDF) binder into a homogenous slurry solution, which was further cast on carbon fiber current collectors (Fuel Cell Store, brand: AvCarb MGL370, thickness: 0.37 mm; diameter: 1.0 cm). The mass ratio between active mass, carbon, and binder was 7:2:1. The electrodes were fully dried in a vacuum drying oven, and the active mass loading was 1–1.5 mg cm^{-2}.

2.4. Electrolyte Preparation

To prepare 30 m $ZnCl_2$ electrolytes, we added 150 mmol $ZnCl_2$ salts into 5 g of deionized water. Note that 1 m means 1 mol kg^{-1} (1 mole of salt per 1 kg of water). We prepared other Zn^{2+} electrolytes using a similar way.

2.5. Battery Assembly and Testing

To characterize the electrochemical performance of the MPc materials, we assembled Zn||MPcs batteries in the Swagelok cell configuration. To evaluate the Zn anode performance, we assembled symmetrical Zn||Zn batteries and asymmetrical Zn||Cu batteries. Glass fiber papers were used as separators, and the amount of electrolyte was ~500 μL.

Galvanostatic charge/discharge curves, rate capability, and cycling performance were tested on the Landt battery cycler (CT3002AU). Cyclic voltammetry curves and electrochemical impedance spectroscopy were tested on the Biologic SP-150 Potentiostat.

3. Results

Figure 1a,b illustrate the crystal structures of the MPc compounds, which crystallize in a triclinic space group characterized by the parameters of a = 12.89 Å, b = 3.77 Å, c = 12.06 Å (α = 96.22°, β = 90.62°, γ = 90.32°), and a unit cell volume of approximately 582 $Å^3$. This expansive structure provides ample interstitial sites and pathways for ion diffusion, which is advantageous for insertion redox reactions. The transition metal lies in the center of MPc structure, which is coordinated by a macrocyclic aromatic phthalocyanine ligand. The conjugated aromatic rings contribute to the good electronic conductivity of the material, thus promoting efficient charge transfer within the cathode.

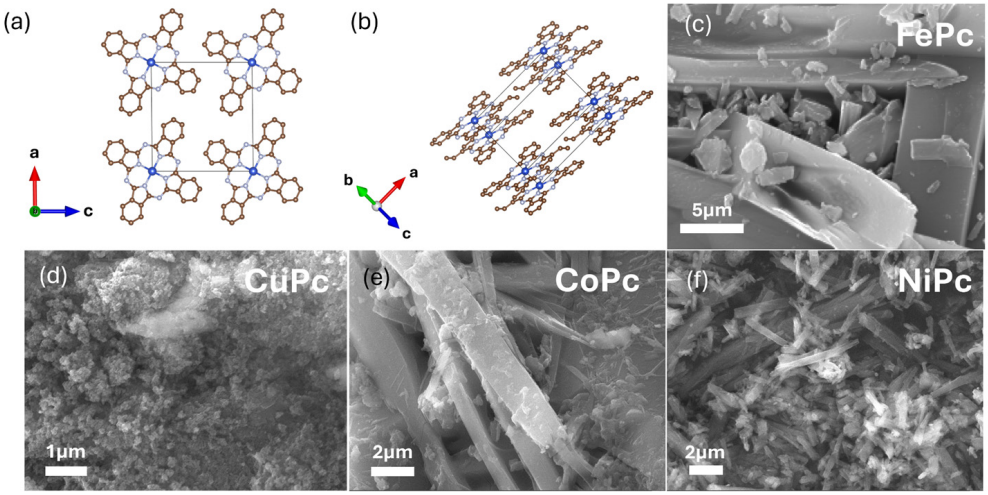

Figure 1. Physical characterization of these MPc compounds. (**a**,**b**) Crystal structures; (**c**–**f**) SEM images of iron, copper, cobalt, and nickel phthalocyanine, respectively.

The transition metal center not only influences the MPcs visual colors (Figure S2) but also affects their morphological tendencies. As shown in Figure 1c,d, these compounds (iron, cobalt, and nickel) tend to grow into fiber-like morphologies, as evidenced by scanning electron microscopy. Different scale bars are used to better show their morphological features and particle size. The fibrous structure can facilitate the ion and electron conduction along the fiber axis. Among them, iron phthalocyanine (Fe-Pc) exhibits the largest particle size, which may correlate with its robust coordination, crystal lattice, and growth conditions. In contrast, copper phthalocyanine (Cu-Pc) appears as nano-sized particles, possibly due to the use of $CuCl_2$ as the salt. Additionally, all these materials exhibit a high crystallinity and chemical purity, as indicated by X-ray diffraction patterns (Figures S3 and S4). The sharp and well-defined diffraction peaks suggest the absence of impurities and demonstrate the structural integrity of the MPc compounds. Energy dispersive X-ray spectroscopy (EDS) mapping analysis further corroborates the high purity (Figure S5).

Many electrodes face the challenge of material dissolution in diluted aqueous electrolytes [38]. To mitigate this issue, we utilize 30 m $ZnCl_2$ WiS electrolyte (1 m = 1 mol kg^{-1}) to better evaluate the electrochemical performance of MPcs. Of note, the 30 m $ZnCl_2$ electrolyte is also beneficial for the Zn metal plating reversibility (Figures S6 and S7). Figure 2 displays the galvanostatic charge/discharge (GCD) curves at the same current of 50 mA g^{-1}. Evidently, the transition metal center plays a vital role in affecting the electrode performance in capacity, voltage, and cycling.

As shown in Figure 2a, Fe-Pc exhibits well-overlapped GCD curves and delivers a reversible capacity of ~60 mAh g^{-1}. There is an apparent charge/discharge plateau at 1.3/1.0 V, corresponding to an average voltage of ~1.15 V. In comparison, Cu-Pc suffers from fast capacity fading (Figure 2b), likely due to the material dissolution issue. We disassembled the battery after cycling and observed light blue color deposits on the separator (Figure S8). Cu-Pc also shows multiple reaction plateaus or slopes, implying a complicated ion insertion mechanism. Although Co-Pc and Ni-Pc electrodes demonstrate relatively stable cycling, their capacity (20–40 mAh g^{-1}) is inferior to that of Fe-Pc. Therefore, among these phthalocyanines, Fe-Pc would be the most promising cathode for aqueous Zn batteries. In addition, the Fe element is much more abundant and inexpensive than Ni, Co, and Mn.

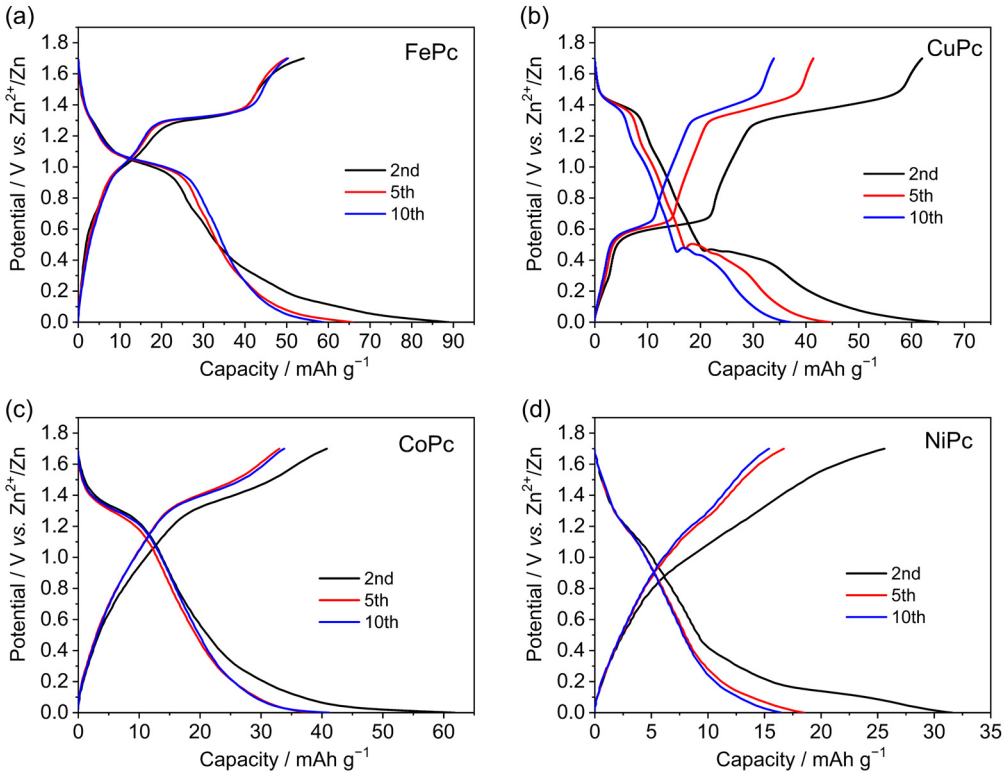

Figure 2. GCD curves of MPc electrodes in the 30 m $ZnCl_2$ electrolyte at 50 mA g^{-1}. (**a**) FePc, (**b**) CuPc, (**c**) CoPc, and (**d**) NiPc.

We further focused on the electrochemical characterizations of the Fe-Pc electrode. As shown in Figure 3a, the capacity after 50 cycles for Fe-Pc is 45 mAh g^{-1}, which is much higher than that of Cu-Pc, Ni-Pc, and Co-Pc. We increased the current to 300 mA g^{-1} and cycled Fe-Pc for more cycling numbers. After 550 cycles, the discharge capacity fades from 37 to 21 mAh g^{-1}, corresponding to a promising capacity retention of 56.7%. The average Coulombic efficiency is calculated as 99.12%, suggesting high reaction reversibility.

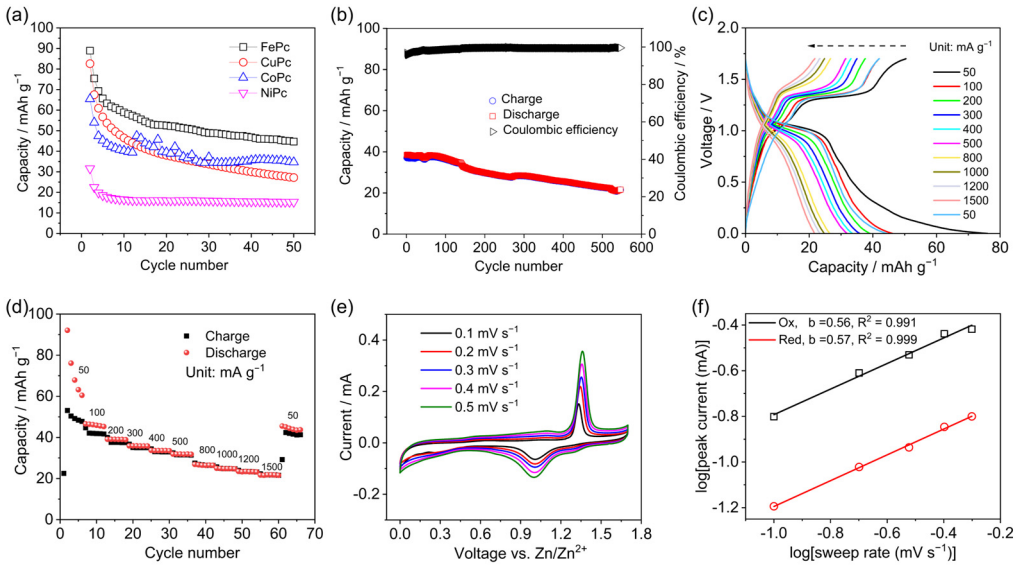

Figure 3. Electrochemical characterizations of the Fe-Pc electrode. (**a**) The cycling comparison between Fe-Pc and other phthalocyanine compounds at 50 mA g^{-1}; (**b**) The long-term cycling of Fe-Pc at 300 mA g^{-1}; (**c**,**d**) The rate performance; (**e**) CV curves at different scanning rates; (**f**) The analysis between log(*i*) and log(*v*).

The stable cycling in Fe-Pc is likely attributed to three key factors. Firstly, the Fe^{2+} ions exhibit stronger coordination with nitrogen atoms in the macrocyclic phthalocyanine rings, leading to intrinsic molecule-level stability [39,40]. Ex-situ XRD tests reveal that the Fe-Pc electrode undergoes a minimal structural change during the charge/discharge (Figure S9). Secondly, the Fe-Pc material exhibits the largest particle size (Figure 1c), which is beneficial to reduce the surface area and mitigate the material dissolution. For comparison, we ball-milled the Fe-Pc material and reduced its particle size. As a result, the ball-milled sample exhibited worse cycling performance than the pristine one (Figure S10), likely due to its smaller size and increased material dissolution. Lastly, the use of 30 m WiS electrolytes can further suppress the material dissolution and boost the cycling life. As shown in Figure S11, the Fe-Pc suffers from fast capacity fading in the conventional 1 m Zn^{2+} ion electrolyte due to the material dissolution (Figure S12). At higher electrolyte concentrations (5 and 15 m), the Fe-Pc electrode still demonstrates an unsatisfactory cycling performance (Figure S13). This comparison highlights the advantages of the 30 m ZnCl2 WiS electrolyte.

Besides stable cycling, Fe-Pc also showcases promising rate capability. As presented in Figure 3c,d, the discharge capacity is 53, 43, 35, 32, 28, 26, 25, 23, and 21 mAh g^{-1} at 50, 100, 200, 300, 400, 500, 800, 1000, and 1200 mA g^{-1}, respectively. Even at 1500 mA g^{-1}, FePc still retains a charge capacity of 20 mAh g^{-1}. Based on its reversible capacity (~50 mAh g^{-1}), we define 1 C rate as 50 mA g^{-1}; therefore, the 1500 mA g^{-1} current density corresponds to a high rate of 30 C. Compared with the literature (Table S1), the Fe-Pc material in this work achieves improved voltage, cycling, and rate performance.

To understand the reaction kinetics, we carried out cyclic voltammetry (CV) studies by using different scanning rates. As shown in Figure 3e, there is one pair of oxidization/reduction peaks at 1.33/1.01 V, which aligns with the observed charge/discharge plateaus. With the increment of the scanning rate, the peak current increases accordingly. It is suggested that the peak current (i) and the scanning rate (v) are correlated by the equation of $i = av^b$, where b equals to 0.5 or 1 if the reaction is diffusion controlled or capacitive [41,42]. We therefore analyzed the relationship between log(i) and log(v) in Figure 3f. As shown, the b value for the cathodic and anodic processes is calculated as 0.56 and 0.57, respectively. This suggests a typical ion insertion process. We also conducted the electrochemical impedance spectroscopy (EIS) analysis of the Fe-Pc battery, which demonstrated a low charge-transfer resistance of ~8.29 Ohm (Figure S14), further corroborating the observed high-rate capability. The fast reaction kinetics also enable the Fe-Pc electrode to work at low-temperature conditions (0 °C, Figure S15). Considering the fundamental research nature of this work, we will conduct more studies toward practical applications, such as high mass loading, limited electrolytes, and full cell assembly.

Based on these results, we conclude that iron phthalocyanine can be utilized as an alternative inexpensive and long-cycling cathode for aqueous Zn batteries. By optimizing electrolyte formulas and material morphology, its electrochemical performance could be further enhanced in future work. Moreover, advanced characterizations will be employed to elucidate the charge-storage mechanism.

4. Conclusions

In this work, we reported the electrochemical performance of various metal phthalocyanine compounds in the $ZnCl_2$ WiS electrolyte. We found that the transition metal center played a vital role in electrochemical performance. Specifically, iron phthalocyanine achieved optimal performance, with the highest capacity, voltage, and cycling stability. Furthermore, it also supported fast-charging capability at ~30 C rate. The improved performance likely resulted from its innate structure, large particle size, and the concentrated

electrolytes. Our work suggested that this abundant and inexpensive iron-based phthalocyanine compound could be a promising cathode for aqueous battery applications.

Supplementary Materials: The following supporting information can be downloaded at https://www.mdpi.com/article/10.3390/batteries11030088/s1.

Author Contributions: Conceptualization, S.Q., D.M.P.C., G.M., and X.W.; investigation, W.H., A.E.A.-C., S.Q., C.O.V., Y.D.A.-T., and L.N.F.-H.; formal analysis, W.H., A.E.A.-C., S.Q., and X.W.; resources, D.M.P.C., G.M., K.G.-N., and X.W.; data curation, W.H., A.E.A.-C., and S.Q.; writing—original draft preparation, W.H. and S.Q.; writing—review and editing, C.O.V. and X.W.; supervision, S.Q., D.M.P.C., G.M., K.G.-N., and X.W.; All authors have read and agreed to the published version of the manuscript.

Funding: The authors thank financial support from the NASA EPSCoR (grant No. 80NSSC23M0189) and NSF Center for the Advancement of Wearable Technologies (grant No. 1849243).

Data Availability Statement: Data are contained within the article.

Conflicts of Interest: The authors declare no conflicts of interest.

References

1. Ji, X. A paradigm of storage batteries. *Energy Environ. Sci.* **2019**, *12*, 3203–3224. [CrossRef]
2. Yang, Y.; Okonkwo, E.G.; Huang, G.; Xu, S.; Sun, W.; He, Y. On the sustainability of lithium-ion battery industry—A review and perspective. *Energy Storage Mater.* **2021**, *36*, 186–212. [CrossRef]
3. Liang, Y.; Yao, Y. Designing modern aqueous batteries. *Nat. Rev. Mater.* **2023**, *8*, 109–122. [CrossRef]
4. Dong, C.; Xu, F.; Chen, L.; Chen, Z.; Cao, Y. Design Strategies for High-Voltage Aqueous Batteries. *Small Struct.* **2021**, *2*, 2100001. [CrossRef]
5. Chang, S.; Qiu, S.; Katiyar, S.; Florez Gomez, J.F.; Feng, Z.; Wu, X. Research Progress on Iron-Based Materials for Aqueous Sodium-Ion Batteries. *Batteries* **2023**, *9*, 349. [CrossRef]
6. Wang, Y.; Yi, J.; Xia, Y. Recent Progress in Aqueous Lithium-Ion Batteries. *Adv. Energy Mater.* **2012**, *2*, 830–840. [CrossRef]
7. Xing, Z.; Wang, S.; Yu, A.; Chen, Z. Aqueous intercalation-type electrode materials for grid-level energy storage: Beyond the limits of lithium and sodium. *Nano Energy* **2018**, *50*, 229–244. [CrossRef]
8. Shangguan, M.; Wang, K.; Zhao, Y.; Xia, L. Tetraethylene Glycol Dimethyl Ether (TEGDME)-Water Hybrid Electrolytes Enable Excellent Cyclability in Aqueous Zn-Ion Batteries. *Batteries* **2023**, *9*, 462. [CrossRef]
9. Ren, W.; Xiong, F.; Fan, Y.; Xiong, Y.; Jian, Z. Hierarchical Copper Sulfide Porous Nanocages for Rechargeable Multivalent-Ion Batteries. *ACS Appl. Mater. Interfaces* **2020**, *12*, 10471–10478. [CrossRef] [PubMed]
10. Xue, T.; Fan, H.J. From aqueous Zn-ion battery to Zn-MnO_2 flow battery: A brief story. *J. Energy Chem.* **2021**, *54*, 194–201. [CrossRef]
11. Li, X.; Chen, Z.; Yang, Y.; Liang, S.; Lu, B.; Zhou, J. The phosphate cathodes for aqueous zinc-ion batteries. *Inorg. Chem. Front.* **2022**, *9*, 3986–3998. [CrossRef]
12. Li, S.; Wei, Z.; Yang, J.; Chen, G.; Zhi, C.; Li, H.; Liu, Z. A High-Energy Four-Electron Zinc Battery Enabled by Evoking Full Electrochemical Activity in Copper Sulfide Electrode. *ACS Nano* **2023**, *17*, 22478–22487. [CrossRef]
13. Hao, J.; Yuan, L.; Zhu, Y.; Bai, X.; Ye, C.; Jiao, Y.; Qiao, S.-Z. Low-cost and Non-flammable Eutectic Electrolytes for Advanced Zn-I_2 Batteries. *Angew. Chem. Int. Ed.* **2023**, *62*, e202310284. [CrossRef] [PubMed]
14. Chen, Q.; Hao, J.; Zhu, Y.; Zhang, S.-J.; Zuo, P.; Zhao, X.; Jaroniec, M.; Qiao, S.-Z. Anti-Swelling Microporous Membrane for High-Capacity and Long-Life Zn−I_2 Batteries. *Angew. Chem. Int. Ed.* **2025**, *64*, e202413703. [CrossRef]
15. Zhang, S.-J.; Hao, J.; Wu, H.; Kao, C.-C.; Chen, Q.; Ye, C.; Qiao, S.-Z. Toward High-Energy-Density Aqueous Zinc–Iodine Batteries: Multielectron Pathways. *ACS Nano* **2024**, *18*, 28557–28574. [CrossRef] [PubMed]
16. Li, Y.; Zhao, J.; Hu, Q.; Hao, T.; Cao, H.; Huang, X.; Liu, Y.; Zhang, Y.; Lin, D.; Tang, Y.; et al. Prussian blue analogs cathodes for aqueous zinc ion batteries. *Mater. Today Energy* **2022**, *29*, 101095. [CrossRef]
17. Nam, K.W.; Kim, H.; Beldjoudi, Y.; Kwon, T.-w.; Kim, D.J.; Stoddart, J.F. Redox-Active Phenanthrenequinone Triangles in Aqueous Rechargeable Zinc Batteries. *J. Am. Chem. Soc.* **2020**, *142*, 2541–2548. [CrossRef]
18. Niu, B.; Wang, J.; Guo, Y.; Li, Z.; Yuan, C.; Ju, A.; Wang, X. Polymers for Aqueous Zinc-Ion Batteries: From Fundamental to Applications Across Core Components. *Adv. Energy Mater.* **2024**, *14*, 2303967. [CrossRef]
19. Wu, F.; Wu, B.; Mu, Y.; Zhou, B.; Zhang, G.; Zeng, L. Metal-Organic Framework-Based Materials in Aqueous Zinc-Ion Batteries. *Int. J. Mol. Sci.* **2023**, *24*, 6041. [CrossRef]

20. Yin, C.; Pan, C.; Liao, X.; Pan, Y.; Yuan, L. Coordinately Unsaturated Manganese-Based Metal–Organic Frameworks as a High-Performance Cathode for Aqueous Zinc-Ion Batteries. *ACS Appl. Mater. Interfaces* **2021**, *13*, 35837–35847. [CrossRef] [PubMed]
21. Ahmed, S.; Ali, A.; Asif, M.; Shim, J.; Park, G. Exploring innovative trends and advancements in rechargeable zinc-air batteries. *Inorg. Chem. Commun.* **2024**, *170*, 113288. [CrossRef]
22. Gounden, D.; Nombona, N.; van Zyl, W.E. Recent advances in phthalocyanines for chemical sensor, non-linear optics (NLO) and energy storage applications. *Coord. Chem. Rev.* **2020**, *420*, 213359. [CrossRef]
23. Ambily, S.; Menon, C.S. Electrical conductivity studies and optical absorption studies in copper phthalocyanine thin films. *Solid State Commun.* **1995**, *94*, 485–487. [CrossRef]
24. Claessens, C.G.; Hahn, U.; Torres, T. Phthalocyanines: From outstanding electronic properties to emerging applications. *Chem. Record* **2008**, *8*, 75–97. [CrossRef] [PubMed]
25. Otero Vélez, C.; Flores, S.Y.; Fonseca, L.F.; Piñero Cruz, D.M. Palladium Phthalocyanine Nanowire-Based Highly Sensitive Sensors for NO_2(g) Detection. *Sensors* **2024**, *24*, 1819. [CrossRef]
26. Zagal, J.H.; Griveau, S.; Silva, J.F.; Nyokong, T.; Bedioui, F. Metallophthalocyanine-based molecular materials as catalysts for electrochemical reactions. *Coord. Chem. Rev.* **2010**, *254*, 2755–2791. [CrossRef]
27. Wang, H.-g.; Wu, Q.; Cheng, L.; Chen, L.; Li, M.; Zhu, G. Porphyrin- and phthalocyanine-based systems for rechargeable batteries. *Energy Storage Mater.* **2022**, *52*, 495–513. [CrossRef]
28. Oni, J.; Ozoemena, K.I. Phthalocyanines in batteries and supercapacitors. *J. Porphyr. Phthalocyanines* **2012**, *16*, 754–760. [CrossRef]
29. Zhao, J.; Zhou, M.; Chen, J.; Tao, L.; Zhang, Q.; Li, Z.; Zhong, S.; Fu, H.; Wang, H.; Wu, L. Phthalocyanine-based covalent organic frameworks as novel anode materials for high-performance lithium-ion/sodium-ion batteries. *Chem. Eng. J.* **2021**, *425*, 131630. [CrossRef]
30. Wang, H.-g.; Wang, H.; Si, Z.; Li, Q.; Wu, Q.; Shao, Q.; Wu, L.; Liu, Y.; Wang, Y.; Song, S.; et al. A Bipolar and Self-Polymerized Phthalocyanine Complex for Fast and Tunable Energy Storage in Dual-Ion Batteries. *Angew. Chem. Int. Ed.* **2019**, *58*, 10204–10208. [CrossRef] [PubMed]
31. Chen, J.; Xu, Y.; Cao, M.; Zhu, C.; Liu, X.; Li, Y.; Zhong, S. A stable 2D nano-columnar sandwich layered phthalocyanine negative electrode for lithium-ion batteries. *J. Power Sources* **2019**, *426*, 169–177. [CrossRef]
32. Hwang, B.; Cheong, J.Y.; Matteini, P.; Yun, T.G. Highly efficient phthalocyanine based aqueous Zn-ion flexible-batteries. *Mater. Lett.* **2022**, *306*, 130954. [CrossRef]
33. Yang, C.; Suo, L.; Borodin, O.; Wang, F.; Sun, W.; Gao, T.; Fan, X.; Hou, S.; Ma, Z.; Amine, K.; et al. Unique aqueous Li-ion/sulfur chemistry with high energy density and reversibility. *Proc. Natl. Acad. Sci. USA* **2017**, *114*, 6197–6202. [CrossRef] [PubMed]
34. Wu, X.; Xu, Y.; Zhang, C.; Leonard, D.P.; Markir, A.; Lu, J.; Ji, X. Reverse Dual-Ion Battery via a $ZnCl_2$ Water-in-Salt Electrolyte. *J. Am. Chem. Soc.* **2019**, *141*, 6338–6344. [CrossRef]
35. Suo, L.; Borodin, O.; Gao, T.; Olguin, M.; Ho, J.; Fan, X.; Luo, C.; Wang, C.; Xu, K. "Water-in-salt" electrolyte enables high-voltage aqueous lithium-ion chemistries. *Science* **2015**, *350*, 938–943. [CrossRef]
36. Qiu, S.; Xu, Y.; Li, X.; Sandstrom, S.K.; Wu, X.; Ji, X. Reinforced potassium and ammonium storage of the polyimide anode in acetate-based water-in-salt electrolytes. *Electrochem. Commun.* **2021**, *122*, 106880. [CrossRef]
37. Zhang, C.; Holoubek, J.; Wu, X.; Daniyar, A.; Zhu, L.; Chen, C.; Leonard, D.P.; Rodríguez-Pérez, I.A.; Jiang, J.-X.; Fang, C.; et al. A $ZnCl_2$ water-in-salt electrolyte for a reversible Zn metal anode. *Chem. Commun.* **2018**, *54*, 14097–14099. [CrossRef]
38. Chao, D.; Zhou, W.; Xie, F.; Ye, C.; Li, H.; Jaroniec, M.; Qiao, S.-Z. Roadmap for advanced aqueous batteries: From design of materials to applications. *Sci. Adv.* **2020**, *6*, eaba4098. [CrossRef]
39. Harris, D.C. *Quantitative Chemical Analysis*; Macmillan: New York, NY, USA, 2010.
40. Baggio, A.R.; Machado, D.F.S.; Carvalho-Silva, V.H.; Paterno, L.G.; de Oliveira, H.C.B. Rovibrational spectroscopic constants of the interaction between ammonia and metallo-phthalocyanines: A theoretical protocol for ammonia sensor design. *Phys. Chem. Chem. Phys.* **2017**, *19*, 10843–10853. [CrossRef]
41. Augustyn, V.; Come, J.; Lowe, M.A.; Kim, J.W.; Taberna, P.-L.; Tolbert, S.H.; Abruña, H.D.; Simon, P.; Dunn, B. High-rate electrochemical energy storage through Li+ intercalation pseudocapacitance. *Nat. Mater.* **2013**, *12*, 518–522. [CrossRef]
42. Augustyn, V.; Simon, P.; Dunn, B. Pseudocapacitive oxide materials for high-rate electrochemical energy storage. *Energy Environ. Sci.* **2014**, *7*, 1597–1614. [CrossRef]